

Modifying the anti-wetting property of butterfly wings and water strider legs by atomic layer deposition coating: surface materials versus geometry

Yong Ding¹, Sheng Xu¹, Yue Zhang², Aurelia C Wang¹,
Melissa H Wang¹, Yonghao Xiu¹, Ching Ping Wong¹ and
Zhong Lin Wang¹

¹ School of Materials Science and Engineering, Georgia Institute of Technology, Atlanta, GA 30332-0245, USA

² Department of Materials Physics and Chemistry, State Key Laboratory for Advanced Metals and Materials, University of Science and Technology Beijing, Beijing 100083, People's Republic of China

E-mail: zhong.wang@mse.gatech.edu

Received 11 May 2008, in final form 12 June 2008

Published 18 July 2008

Online at stacks.iop.org/Nano/19/355708

Abstract

Although butterfly wings and water strider legs have an anti-wetting property, their working conditions are quite different. Water striders, for example, live in a wet environment and their legs need to support their weight and bear the high pressure during motion. In this work, we have focused on the importance of the surface geometrical structures in determining their performance. We have applied an atomic layer deposition technique to coat the surfaces of both butterfly wings and water strider legs with a uniform 30 nm thick hydrophilic Al₂O₃ film. By keeping the surface material the same, we have studied the effect of different surface roughness/structure on their hydrophobic property. After the surface coating, the butterfly wings changed to become hydrophilic, while the water strider legs still remained super-hydrophobic. We suggest that the super-hydrophobic property of the water strider is due to the special shape of the long inclining spindly cone-shaped setae at the surface. The roughness in the surface can enhance the natural tendency to be hydrophobic or hydrophilic, while the roughness in the normal direction of the surface is favorable for forming a composite interface.

1. Introduction

Super-hydrophobicity is a very popular phenomenon in nature, through which lotus leaves are self-cleaning [1], butterflies avoid sticking of their wings [2] and water striders float and move on a water surface [3, 4]. The natural super-hydrophobic surfaces generally have three common features: (a) they are coated by wax or a hydrophobic film; (b) they are decorated by textures such as bumps, pillars, or grooves at a scale of typically a few micrometers; and (c) they have a secondary texture superposed on the first one. Besides surface chemistry, the surface roughness and geometry have a crucial role in affecting the super-hydrophobicity [5, 6].

Two important factors are normally used to characterize the hydrophobicity of a material's surface [7]: the contact angle and the contact angle hysteresis. The contact angle hysteresis is the difference between the advancing and receding contact angles. Although the advancing contact angle in both Wenzel and Cassie states are significantly larger than the Young's angle θ , the hysteresis is dramatically different for the two cases [7]. The hysteresis for the Cassie state, the composite surface situation, is found to be 10–20 times smaller than that for the Wenzel state [8]. This is of practical importance, because a droplet in the Wenzel state will adhere much more easily to its substrate, in contrast to what is expected in a super-hydrophobic situation. In particular, the so-called self-cleaning

effect is totally suppressed by the drop adhesion. In addition, it was shown recently that the friction properties of these materials should be extremely different according to the state: a Cassie state should lead to a strong reduction of the friction properties, while a Wenzel state has greater friction properties than that for a flat hydrophobic material [9]. If anti-wetting is desired, effort is needed to keep the surface in the Cassie regime to form a composite interface instead of the Wenzel one [10].

In a composite surface, the difference of the pressures in liquid and in air pocket can be revealed by the curvature R of the liquid/air interface by the Laplace law: $\Delta p = 2\gamma_{LV}/R$, where γ_{LV} is the liquid/vapor surface tension. The Laplace pressure is introduced by the liquid surface tension [11]. The largest Laplace pressure that the droplet can bear is calculated based on the detailed geometry of the texture, Young's angle θ , and γ_{LV} [12]. On increasing of the size and weight of the water droplet, the force coming from Laplace pressure can be used to balance the gravity to keep the air pocket. Therefore, in order to stabilize the composite surface, choosing a special surface geometry to get the largest Laplace pressure with designed force direction should be a potential approach.

Butterfly wings and water striders have attracted a lot of attention due to their naturally developed super-hydrophobicity. For example, the work of Jiang's group on butterfly wings revealed that the direction-dependent arrangement of nano-tips on ridging nano-strips and micro-scales overlapping on the wings introduce anisotropic adhesion [2]. Using a molding technique, the surface of a water strider was successfully replicated. The dominant role of the surface topography was further emphasized by the super-hydrophobic properties of the replica [13]. In order to better design and create super-hydrophobic/super-hydrophilic surfaces [14], in this work, we compared the structure difference of these two systems, butterfly wing and water strider. Using an atomic layer deposition (ALD) technique to coat the surfaces of both butterfly wings and water strider legs with a uniform 30 nm thick hydrophilic Al_2O_3 film, we kept the surface material of both structures the same. Due to the merit of ALD technique, the surface structure of each system was maintained after coating [15, 16]. Thereafter we studied the effect of different surface roughness/structure on their hydrophobic property. After the surface coating, the butterfly wings changed to become hydrophilic, while the water strider legs still remained super-hydrophobic. We have designed a set of experiments to investigate such structure-related phenomenon. Our results suggest that the super-hydrophobic property of the water strider is due to the long inclining spindly cone-shaped setae at the surface. The roughness in the surface can enhance the natural tendency to be hydrophobic or hydrophilic, while the roughness in the normal direction of the surface is favorable for forming a composite interface, which means the formation of the Cassie state.

2. Experimental details

The butterflies were *Morpho peleides*, provided by the Day Butterfly Center in Callaway Gardens. The water striders

were captured from a local pond in Atlanta. The atomic layer deposition (ALD) was performed in a Savannah 100 Atomic Layer Deposition system manufactured by Cambridge NanoTech Inc. Two precursors for Al_2O_3 deposition were 99.9999% $\text{Al}(\text{CH}_3)_3$ (TMA) purchased from Aldrich, and deionized H_2O , with a resistivity of $\sim 18 \text{ M}\Omega$. During the deposition, the thickness of the Al_2O_3 layer could be controlled very well by varying the number of cycles of deposition, where the growth rate was 0.1 nm per cycle. With such a high precision of control, the Al_2O_3 layer covers the entire biological sample uniformly and completely. Since the coating layer was so thin, the coating does not change the geometry of the sample.

Contact angle measurements were performed using a Rame-Hart goniometer that had a charge-coupled device (CCD) camera equipped for image recording. A LEO 1530 scanning electron microscope (SEM) was used to characterize the surface morphology of the butterfly wings and water strider legs.

3. Results and discussion

Atomic layer deposition (ALD) is ideally suited for a uniform, controlled and complete coating over the entire biological sample at low temperature. The ALD coating changes only the surface chemistry/material while preserving the detailed texture/geometry structure. Figures 1(a)–(c) display SEM images of a 30 nm thick Al_2O_3 coated butterfly wing at different magnifications. The butterfly wing surface is covered entirely, uniformly and completely by the amorphous inorganic layer, as shown in figure 1(a). The typical dimension of the scale is $\sim 150 \mu\text{m}$ in length and $\sim 60 \mu\text{m}$ in width. Thirty five to forty rows of ridges align on the scale surface with almost an identical interspacing. The height of the ridges, h , is $\sim 1 \mu\text{m}$ and the distance L between them is $\sim 1.6 \mu\text{m}$, as depicted in figure 1(c). The measured contact angles (one image is shown in figure 1(d)) on the natural butterfly wings are listed in table 1. The static Young's contact angle of flat Al_2O_3 surface was measured to be $70.0^\circ \pm 5^\circ$, which will be described in detail below. After coating Al_2O_3 (energy dispersive x-ray spectroscopy (EDS) confirmed the successful coating), the static contact angle of the butterfly wing in figure 1(e) was measured as 38° . It is obviously that, after coating, the butterfly wing changes from the Cassie state to the Wenzel state. Based on the static contact angle and Young's contact angle of Al_2O_3 , the roughness r is calculated to be ~ 2.3 , which is in good agreement with the measured roughness of 2.25 based on the SEM images, where $r = \frac{L+2h}{L}$.

Figures 2(a) and (b) are SEM images of a natural and a 30 nm thick Al_2O_3 coated water strider leg, respectively. The spindly setae are packed on the surface with an inclining angle of $\sim 30^\circ$, as shown in figure 2(c). The density of the setae in the surface is $\sim 2 \times 10^5 \text{ cm}^{-2}$. The diameter of one leg is 150–200 μm , while the seta is 2–5 μm in diameter and 30–50 μm in length. The EDS spectra acquired from both natural and Al_2O_3 coated water strider legs are displayed in figure 2(d), which proved the successful coating of the Al_2O_3 thin film on the surface.

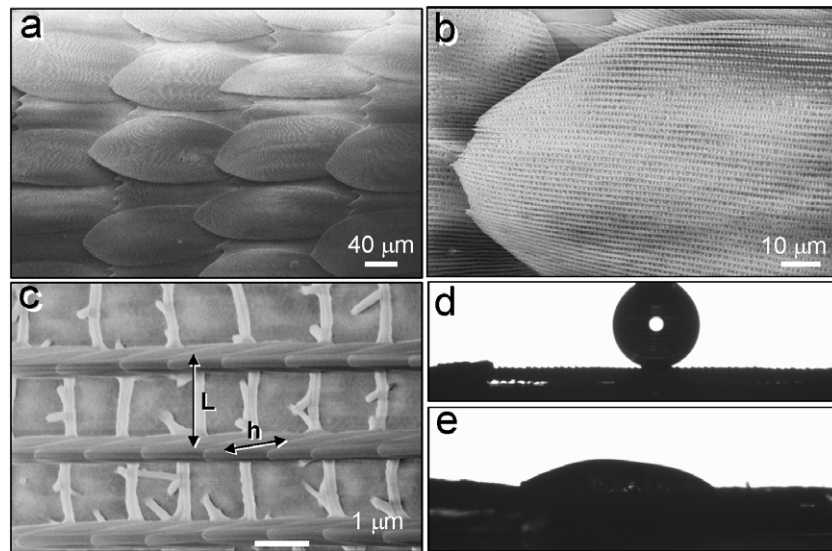


Figure 1. (a)–(c) SEM images of butterfly wings at different magnifications. ((d) and (e)) The switching from hydrophobic to hydrophilic nature of the wing surface after coating with 30 nm thick Al_2O_3 film.

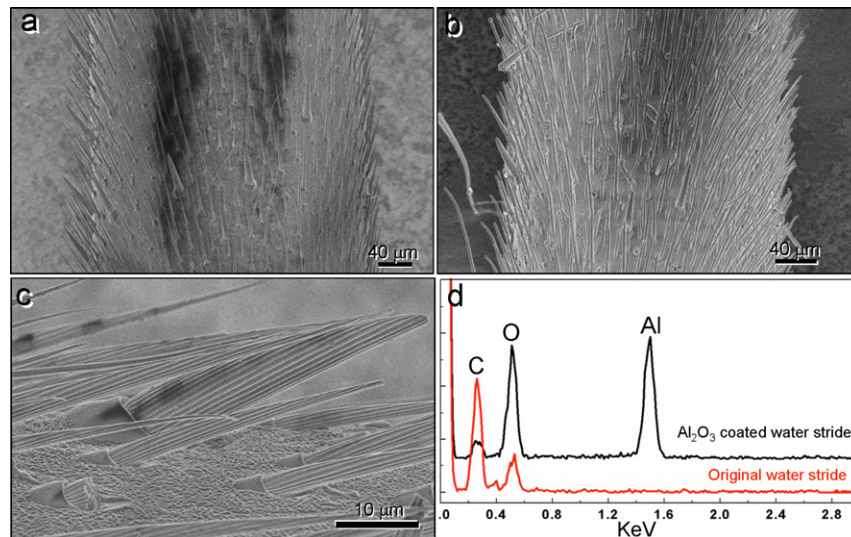


Figure 2. ((a), (b)) SEM images of natural and Al_2O_3 coated water strider legs, respectively. (c) SEM image of an Al_2O_3 coated water strider leg. (d) EDS spectra acquired from a natural water strider leg and an Al_2O_3 coated one.

(This figure is in colour only in the electronic version)

Table 1. Contact angle data for butterfly wings and water strider legs.

	Before alumina coating			After alumina coating		
	θ_A (deg)	θ_R (deg)	Hysteresis (deg)	θ_A (deg)	θ_R (deg)	Hysteresis (deg)
Butterfly wing	166.0	155.3	10.7	38.0		Not measurable
Water strider leg	172.3	172.3	~0.0	147.3	112.0	35.3 ^a
				159.6	114.2	45.4 ^b

^a Along the seta's inclining direction.

^b Against the seta's inclining direction.

Images presenting the static apparent contact angles along and perpendicular to the legs before Al_2O_3 coating are displayed in figures 3(a) and (b), respectively. After coating, the corresponding images are displayed in figures 3(a')

and (b'). In contrast to the case for butterfly wings, there is no obvious difference in hydrophobicity before and after the Al_2O_3 coating. The contact angles observed along and perpendicular to the legs are both larger than 150° , showing

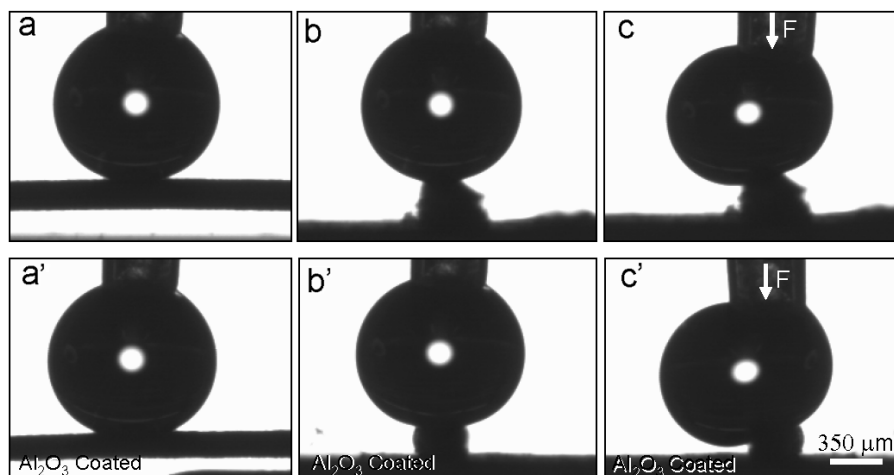


Figure 3. ((a), (b)) Contact angles measured along and perpendicular to the leg of a natural water strider. (c) Same as (b), except a downward pressure was applied on the droplet. ((a'), (b'), (c')) the corresponding cases as for (a), (b), (c), respectively, for a leg coated with Al_2O_3 . The diameter of the water droplet is ~ 1.8 mm.

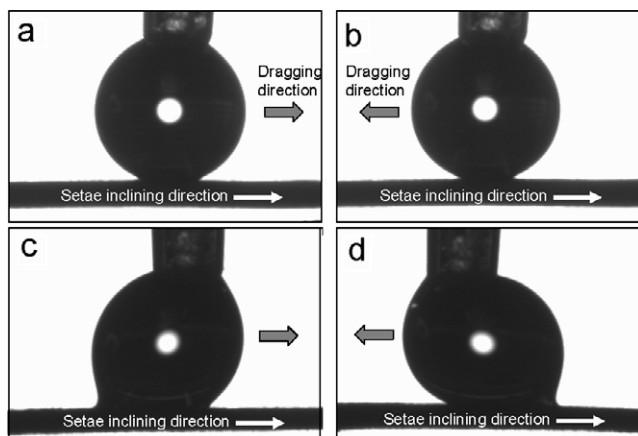


Figure 4. Contact angle hysteresis of a water strider leg before ((a), (b)) and after ((c), (d)) coating with Al_2O_3 . The difference in hysteresis reflects the anisotropic effect as the water drop is dragged along and against the seta's inclining direction. The diameter of the water droplet is ~ 1.8 mm.

super-hydrophobicity. Even if we push the water droplet to increase the downward pressure, both legs tend to repulse the droplet, as shown in figures 3(c) and (c'). The large contact angle indicates that the surface after coating is still in the Cassie state, although it is a metastable state.

By dragging a $3 \mu\text{m}$ water droplet in one direction along a water strider leg, we measured the advancing and receding angles, and then the contact angle hysteresis, as displayed in table 1. The different contact angle hysteresis between the natural and coated legs is displayed in figure 4. Before coating, the hysteresis was less than 1.0° , regardless of whether along the seta inclining direction or against the inclining direction. After coating, the hysteresis increased to $\sim 35.3^\circ$ (figure 4(c)) and $\sim 45.4^\circ$ (figure 4(d)), as displayed in table 1, for moving along and against the seta's inclining direction, respectively.

The above experiments show that, after coating with a thin layer of hydrophilic Al_2O_3 , the butterfly wings changed from

being super-hydrophobic to hydrophilic, corresponding to the change from the Cassie state to the Wenzel state [17], while the water strider legs still remained in the super-hydrophobic Cassie state. We know that the roughness of a butterfly wing is mostly in the surface plane, and that the wing is uniform in the direction perpendicular to the surface plane (seeing figure 1(c)), while the water strider leg and its setae are close to cylindrical, which means that the roughness is three dimensional. To examine the influence of the overall profile shape of an object on its anti-wetting property, we have designed an experiment. We have chosen thin copper wires with the same Al_2O_3 coating by ALD technique under the same experimental conditions to investigate the interface configurations. In order to capture the clear liquid/solid interface images using the CCD camera we have, the diameter of the wire was kept to the smallest possible that was still resolvable. The suitable diameter of the wire we chose was $150 \mu\text{m}$.

By dropping a $3 \mu\text{m}$ water droplet on an Al_2O_3 coated flat Si substrate as displayed in figure 5(a), we can approximately take the measured contact angle of 70.0° as the static Young's angle of the flat Al_2O_3 surface. This proves the hydrophilicity of the coating layer. The experiment design of a single coated wire is depicted in figure 5(b). Although the wire is coated by a hydrophilic layer of Al_2O_3 , the water droplet did not fully soak the wire. Instead, as shown in figure 5(c), a clear liquid/solid interface was built up even when we gave a downward pressure to the droplet. Based on the droplet curvature as displayed in the inset of figure 5(c), we can identify that the Laplace pressure is upward. This means that due to the round shape, the liquid surface tension, e.g., the capillary effect [12, 18], works upward to balance the droplet weight and the external applied pressure.

Furthermore, a similar experiment was done for an array of Al_2O_3 coated wires array, as shown in figure 5(d). Using different droplet sizes, the interface images observed along the wire direction were recorded; they are displayed in figures 5(e)–(g). The air pocket can be clearly observed in

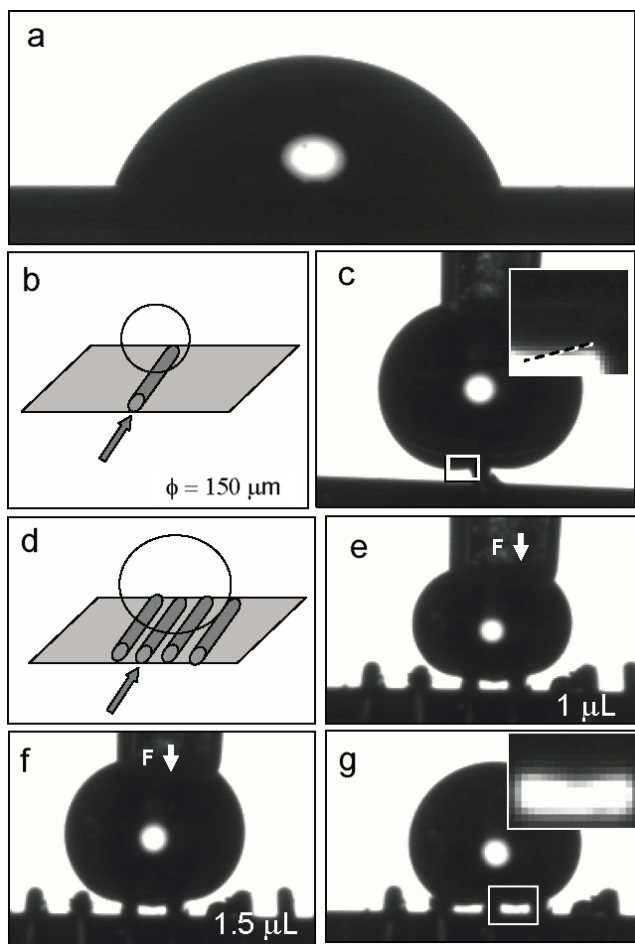


Figure 5. (a) The Young's contact angle of an Al_2O_3 film coated on a flat Si substrate. ((b) and (c)) A schematic and practical image of a water droplet on a single Cu wire coated with Al_2O_3 , for simulating the curvature effect of a seta. ((d)–(g)) A water droplet on an array of wires coated with Al_2O_3 . The upward Laplace pressure can be identified by the curvature inserted in (g). As mentioned in (b), the diameter of the Cu wire is $\sim 150 \mu\text{m}$.

between two nearby wires. The inset in figure 5(g) gives the clear curvature of the droplet, which indicates the upward Laplace pressure. We pushed the droplet downward, and with the increase of apparent contact angle, the droplet preferred to span to nearby wires instead of falling down to fill in the air cavities.

The effect of the rounded shape in the wettability can be explained by the models shown in figures 6(a) and (b), which are looking along the wire. In the following discussions on the contact angles, we are based on the structure of a three-phase contact line. Two types of force act on the suspended water droplet: one is the gravity of the droplet, and the other is from the Laplace pressure introduced by the surface tension of the water [19–21]. If both forces work downward, then the water droplet will collapse and sweep away the downside air. In order to make the suspended water droplet stable, the Laplace pressure (from surface tension) of the water must point upward, which means that the contact angle plus inclining angle α of the surface must be larger than 180° . The direction of the Laplace pressure introduced by the surface tension can

be uniquely identified by the droplet curvatures. The measured local contact angles can be larger than (see figure 6(a)) and smaller than (see figure 6(b)) 90° , depending on the local contact line. If the surface of the wire is made of a hydrophilic material, which means that the advancing angle is less than 90° , the case in figure 6(a) is unstable because the local contact angle $\theta_{\alpha 2} + \alpha < 180^\circ$, which means that the direction of Laplace pressure is the same as that of gravity. After the droplet falls down to touch the bottom half of the wire as shown in figure 6(b), although the local contact angle $\theta_{\alpha 1}$ is still less than 90° , the inclining angle is now much increased; therefore $\theta_{\alpha 2} + \alpha > 180^\circ$. There exists a critical position at which $\theta_{\alpha 1} \leq$ advancing angle of the materials and advancing angle plus inclining angle $\alpha = 180^\circ$; thus, the droplet starts to be pinned. The alumina coated copper wires as shown in figure 5 belong to such a case.

Alternatively, if the wire surface is coated by a hydrophobic material, which means that the Young angle is $>90^\circ$, the water droplet can be stably pinned at one of the locations in the upper half circle of the wire to satisfy the condition of contact angle $\theta_{\alpha 2} <$ advancing angle of the material and satisfy Young's angle θ plus inclining angle $\alpha > 180^\circ$ to get upward Laplace pressure. Therefore, regardless of whether the coating material is hydrophobic or hydrophilic, there is always a stable pinning position to pin the droplet and preserve the air cavity at the bottom of the wire. Accordingly, the setae in water strider legs can easily trap the air pockets by adjusting the water–liquid contact lines to stabilize the Cassie state, resulting in a better anti-wetting property. It is obvious that the hydrophilic surface has a much larger liquid/solid interface compared to the hydrophobic one. The increased water–surface contact area can be the reason that the contact angle hysteresis is larger for the Al_2O_3 coated legs than that of the natural ones, as described in figure 4.

The situation for a butterfly wing is different. The roughness of the butterfly wing is mostly in the surface plane, e.g., two-dimensional, but the wing is fairly uniformly in the normal direction perpendicular to the wing surface. A natural wing is hydrophobic (figure 6(c)) with advancing angle + inclining angle $> 180^\circ$. Once coated with Al_2O_3 , the surface becomes hydrophilic (figure 6(d)). In such a case, the capillary effect will draw the water droplet downward into the cavities following the Wenzel state, and surface wetting occurs.

Our experimental results are consistent with the theoretical works on the super-hydrophobicity on hydrophilic substrates [22, 23]. The special topology of water strider legs give an ideal model to trap the air under the water drop, regardless of whether the surface material is hydrophobic or hydrophilic. Although butterfly wings and water strider legs both show super-hydrophobic properties with wax coating, only water strider legs still keep the properties after uniform Al_2O_3 coating. This means that the surface topography of the water strider legs is more suitable in anti-wetting design than that of butterfly wings.

The above discussion has shown that the super-hydrophobic/anti-wetting property is dramatically enhanced by the surface texture of water striders, although the surface chemistry is another key factor in determining such a

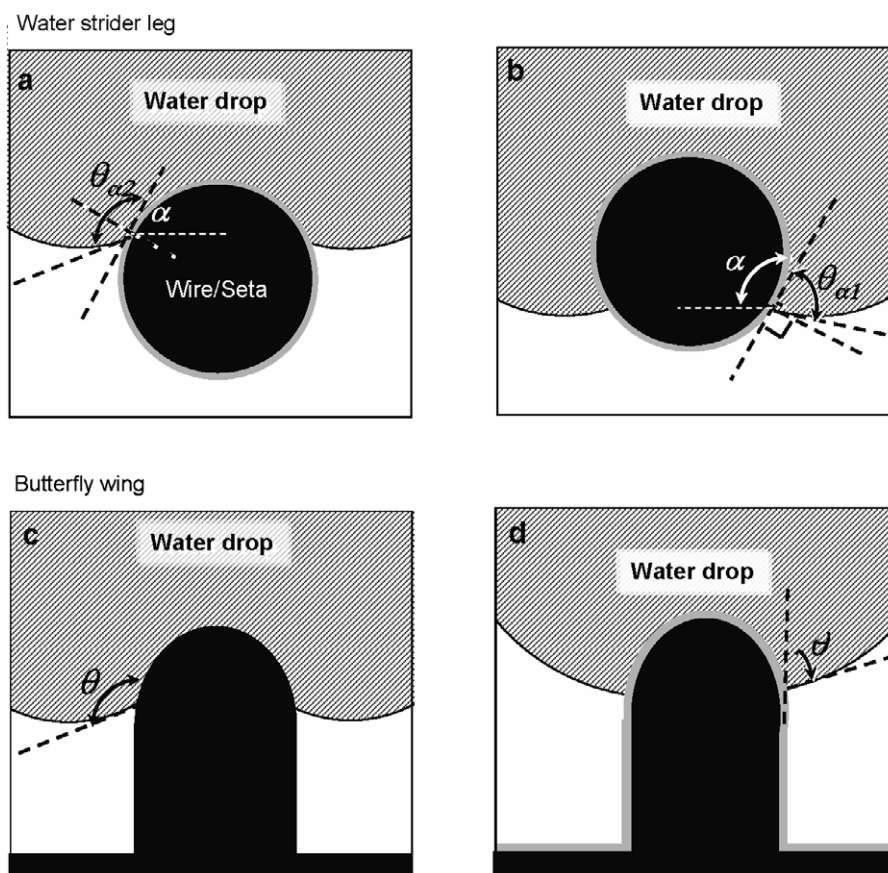


Figure 6. ((a), (b)) Schematic models showing the contacts of a water droplet with a cylindrical wire that simulates the seta on the water strider leg at upper and lower half surfaces, respectively. ((c), (d)) Schematic models showing the contacts of a water droplet with a vertical walled structure that simulates the fine structure on the surface of a butterfly wing for a natural and Al_2O_3 coated butterfly wing, respectively.

property [24]. There is another important phenomenon, in that the setae in the leg surface have a cone shape instead of uniform cylindrical shape and inclining angle around 30° . This may be related to the anisotropic wetting phenomenon [2, 25–27].

4. Summary

By comparing the wettability changes of butterfly wings and water strider legs before and after ALD coating with a hydrophilic Al_2O_3 layer, the structural superiority of water strider legs has been revealed. The Al_2O_3 coating makes butterfly wings change from super-hydrophobic (Cassie state) to hydrophilic (Wenzel state), while the water strider legs remain super-hydrophobic even under applied pressure. The greater anti-wetting property of the water strider is likely due to the round shape of the inclining setae at its surface, which prefer to trap the air pocket under the water drops to form a composite surface. We have obtained evidence that the cylindrical-shaped structures lying on the surface can stabilize the Cassie state. If the water droplet size is larger than the scale of the surface roughness, by adjusting the contact lines at the interface, regardless of whether the surface is hydrophobic or hydrophilic, the system prefers to trap air to form a composite interface. The surface wettability in the case when the drop size and surface roughness are of the same magnitude has been

discussed in [28]. The roughness in the surface can enhance the natural tendency to be hydrophobic or hydrophilic, while the roughness in the normal direction of the surface is favorable for the Cassie state [29]. This study demonstrates an outstanding example of exploring the nature of the anti-wetting property of animals and plants.

Acknowledgments

We thank Jessica C Wang for help in acquiring the water strider samples. This work was supported by DOE BES (DE-FG02-07ER46394), NSF (DMS 0706436), NSF of China (50620120439) and MOST of China (2006DFB51000).

References

- [1] Feng L, Li S H, Li Y S, Li H J, Zhang L J, Zhai J, Song Y L, Liu B Q, Jiang L and Zhu D B 2002 *Adv. Mater.* **14** 1857–60
- [2] Zheng Y M, Gao X F and Jiang L 2007 *Soft Matter* **3** 178–82
- [3] Gao X F and Jiang L 2004 *Nature* **432** 36
- [4] Hu D L, Chan B and Bush J W M 2003 *Nature* **424** 663–6
- [5] Bico J, Marzolin C and Quere D 1999 *Europhys. Lett.* **47** 220–6
- [6] Herminghaus S 2000 *Europhys. Lett.* **52** 165–70
- [7] Quere D 2005 *Rep. Prog. Phys.* **68** 2495–532
- [8] Lafuma A and Quere D 2003 *Nat. Mater.* **2** 457–60

- [9] Cottin-Bizonne C, Barrat J L, Bocquet L and Charlaix E 2003 *Nat. Mater.* **2** 237–40
- [10] Oner D and McCarthy T J 2000 *Langmuir* **16** 7777–82
- [11] Arthur W and Adamson A P G 1997 *Physical Chemistry of Surfaces* 6th edn (New York: Wiley–Interscience) chapter X
- [12] Tsori Y 2006 *Langmuir* **22** 8860–3
- [13] Goodwyn P P, Souza E D, Fujisaki K and Gorb S 2008 *Acta Biomater.* **4** 766–70
- [14] Feng X J and Jiang L 2006 *Adv. Mater.* **18** 3063–78
- [15] Ritala M, Kukli K, Rahtu A, Raisanen P I, Leskela M, Sajavaara T and Keinonen J 2000 *Science* **288** 319–21
- [16] George S M, Ott A W and Klaus J W 1996 *J. Phys. Chem.* **100** 13121–31
- [17] Bico J, Thiele U and Quere D 2002 *Colloids Surf. A* **206** 41–6
- [18] Xiu Y H, Zhu L B, Hess D W and Wong C P 2007 *Nano Lett.* **7** 3388–93
- [19] Extrand C W 2002 *Langmuir* **18** 7991–9
- [20] Extrand C W 2004 *Langmuir* **20** 5013–8
- [21] Extrand C W 2005 *Langmuir* **21** 10370–4
- [22] Liu J L, Feng X Q, Wang G F and Yu S W 2007 *J. Phys.: Condens. Matter* **19** 356002
- [23] Bhushan B and Jung Y C 2008 *J. Phys.: Condens. Matter* **20** 225010
- [24] Shi F, Niu J, Liu J L, Liu F, Wang Z Q, Feng X Q and Zhang X 2007 *Adv. Mater.* **19** 2257–61
- [25] Chung J Y, Youngblood J P and Stafford C M 2007 *Soft Matter* **3** 1163–9
- [26] Chen Y, He B, Lee J H and Patankar N A 2005 *J. Colloid Interface Sci.* **281** 458–64
- [27] Zhao Y, Lu Q H, Li M and Li X 2007 *Langmuir* **23** 6212–7
- [28] Cheng Y T, Rodak D E, Angelopoulos A and Gacek T 2005 *Appl. Phys. Lett.* **87** 194112
- [29] Nosonovsky M 2007 *Langmuir* **23** 3157–61